



Available online at www.sciencedirect.com

ScienceDirect

NUCLEAR
PHYSICS

A

ELSEVIER

Nuclear Physics A 982 (2019) 403–406

www.elsevier.com/locate/nuclphysa

Measurement of longitudinal decorrelation of anisotropic flow V_2 and V_3 in 200 GeV Au+Au collisions at STAR

Maowu Nie (for the STAR Collaboration)

Shanghai Institute of Applied Physics, Chinese Academy of Sciences, Shanghai 201800, China

Department of Chemistry, Stony Brook University, Stony Brook, NY 11794, USA

Abstract

Measurements of longitudinal flow decorrelations for charged particles are presented in the pseudorapidity range $|\eta| < 1$ using a reference detector at $2.5 < \eta_{\text{ref}} < 4$ in Au+Au collisions at $\sqrt{s_{NN}} = 200$ GeV by STAR. The factorization ratio (r_n), which represents the magnitude of decorrelation, shows a strong centrality dependence for the second-order factorization ratio (r_2), while a weak centrality dependence for the third-order factorization ratio (r_3). Furthermore, the decorrelation measured at RHIC energy is found to be stronger than that at the LHC energies. Current ideal and viscous hydrodynamic models fail to simultaneously describe the longitudinal flow decorrelations measured at RHIC and the LHC energies.

Keywords: flow decorrelation, longitudinal dynamics, STAR

1. Introduction

Initial-state fluctuations in the transverse plane in the heavy-ion collisions are essential for the understanding of the final-state dynamics of multiparton interactions in Quark-Gluon Plasma. However, most of these studies assumed that the initial condition and space-time evolution of the collisions are boost-invariant in the longitudinal direction. It is recently realized that the longitudinal fluctuations could have a similar important role for the entire space-time evolution of the medium produced in heavy-ion collisions [1–3].

The decorrelation of flow harmonics, V_n , in the longitudinal direction explores the non-boost-invariant nature of the initial-collision geometry and final-state collective dynamics. The decorrelations were first measured at the LHC [4, 5], but are predicted by several (3+1)D hydrodynamic models to be stronger for lower $\sqrt{s_{NN}}$ at RHIC due to the smaller number of initial partons and shorter string length at lower energies [6]. In this proceeding, we present the new measurements of flow decorrelation in Au+Au at $\sqrt{s_{NN}} = 200$ GeV with the STAR detector. Comparisons with results from the LHC and calculations from different models for different centralities are discussed.

2. Analysis method

The azimuthal anisotropy of the particle production in an event is described by harmonic flow vector, $\mathbf{V}_n = v_n e^{in\Psi_n}$, where v_n and Ψ_n are the magnitude and phase (or event plane), respectively. Experimentally,

<https://doi.org/10.1016/j.nuclphysa.2018.09.068>

0375-9474/© 2018 Published by Elsevier B.V.

This is an open access article under the CC BY-NC-ND license (<http://creativecommons.org/licenses/by-nc-nd/4.0/>).

\mathbf{V}_n is estimated from the observed per-particle flow vector, $\mathbf{q}_n \equiv \sum \omega_i e^{in\phi_i} / \sum \omega_i$, where the sum runs over all charged particles in the phase-space sample and ω_i is the weight assigned to the i^{th} particle. The flow vector, \mathbf{q}_n , deviates from \mathbf{V}_n due to non-flow contribution and statistical fluctuations. By requiring a large pseudorapidity gap, the non-flow contribution can effectively suppressed and the statistical fluctuation drops after event average. The correlation between \mathbf{V}_n from two pseudorapidity intervals can then be estimated with the observed flow vector \mathbf{q}_n :

$$\langle \mathbf{q}_n(\eta) \mathbf{q}_n^*(\eta_{\text{ref}}) \rangle = \langle \mathbf{V}_n(\eta) \mathbf{V}_n^*(\eta_{\text{ref}}) \rangle \quad (1)$$

The factorization ratio, r_n , is used to measure the decorrelation between η and $-\eta$ relative to a common reference η_{ref} [4]. It is defined as Eq. 2. The observable is sensitive to the event-by-event fluctuations of the initial condition in the longitudinal direction. If flow harmonics from two-particle correlations factorize into single-particle flow harmonics, then the value of r_n is expected to equal to unit. Therefore $r_n \neq 1$ implies the breakdown of the two-particle correlation factorization.

$$r_n(\eta) = \frac{\langle \mathbf{q}_n(-\eta) \mathbf{q}_n^*(\eta_{\text{ref}}) \rangle}{\langle \mathbf{q}_n(\eta) \mathbf{q}_n^*(\eta_{\text{ref}}) \rangle} = \frac{\langle v_n(-\eta) v_n(\eta_{\text{ref}}) \cos n(\Psi_n(-\eta) - \Psi_n(\eta_{\text{ref}})) \rangle}{\langle v_n(\eta) v_n(\eta_{\text{ref}}) \cos n(\Psi_n(\eta) - \Psi_n(\eta_{\text{ref}})) \rangle} \quad (2)$$

In this analysis, the measurements are performed using charged particles with $0.4 < p_T < 4$ GeV/c from the Time Projection Chamber (TPC, $|\eta| < 1$), and the reference flow vector is calculated from the Forward Meson Spectrometer (FMS, $2.5 < |\eta_{\text{ref}}| < 4$) for the $\sqrt{s_{NN}} = 200$ GeV Au+Au collisions. The systematic uncertainties for the observables are estimated using positive track and negative tracks, respectively, and indicated with hollowed boxes.

3. Results and discussion

Figure 1 shows the factorization ratio r_2 and r_3 as a function of η , averaged over $0.4 < p_T < 4$ GeV/c for 20-30% central Au+Au collisions. Both r_2 and r_3 decrease linearly with η increasing. This decreasing trend could be well described by a linear fit.

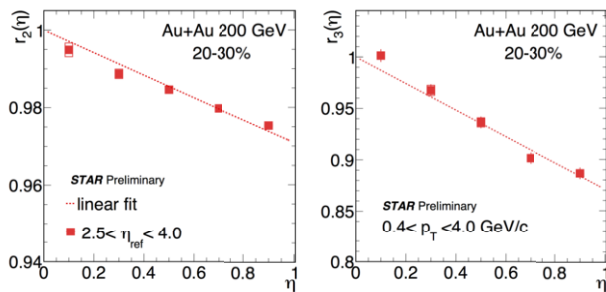


Fig. 1. (Left panel) The factorization ratio r_2 as a function of η , averaged over $0.4 < p_T < 4$ GeV/c for 20-30% Au+Au collisions, The error bars and hollowed boxes are statistical and systematic uncertainties, respectively. (Right panel) Same style as r_2 , but for r_3 .

The similar behavior is also observed for the other centralities. To study the centrality dependence, the r_n is parameterized with a linear function, $r_n = 1 - 2F_n\eta$. Figure 2 shows the centrality dependence of F_n in terms of N_{part} , which quantifies the strength of the decorrelation effect. F_2 shows a clearly centrality dependence, where the decorrelation effect is the weakest at midcentral collisions. F_3 shows weak centrality dependence.

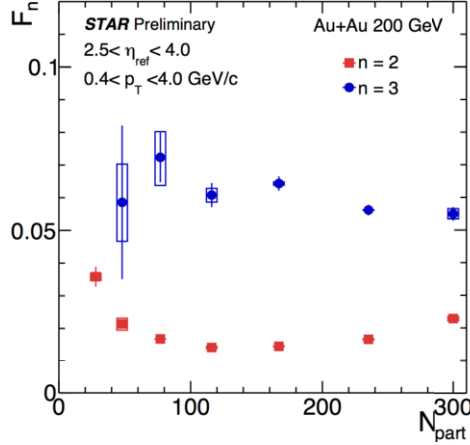


Fig. 2. Centrality dependence of F_n for 200 GeV Au+Au collisions. The error bars and hollowed boxes are statistical and systematic uncertainties, respectively.

Since the beam rapidity has energy dependence, a direct comparison between the decorrelation results at RHIC energy with the results at the LHC energies could be biased by the reach of beam rapidity y_{beam} , therefore, r_n are plotted as a function of normalized pseudorapidity η/y_{beam} as shown in Fig. 3. r_2 (top panel) is plotted in various centrality intervals at three collision energies, the markers are the experimental measurements [5]. A clear energy dependence is observed, where the results at $\sqrt{s_{NN}} = 200 \text{ GeV}$ and $\sqrt{s_{NN}} = 5.02 \text{ TeV}$ show the strongest and the weakest decorrelation effects, respectively. The decorrelation difference between lower and higher collision energies also shows a centrality dependence. The (3+1)D CLVisc ideal hydrodynamics [7], which is tuned to describe the decorrelation effect at $\sqrt{s_{NN}} = 2.76 \text{ TeV}$ Pb+Pb collisions can quantitatively describe the data [6]. However, the ideal hydrodynamics overestimates the effect at $\sqrt{s_{NN}} = 200 \text{ GeV}$ Au+Au collisions. The hydrodynamic calculations also capture the deviation between higher and lower $\sqrt{s_{NN}}$. With a shear viscosity to entropy density ratio $\eta/s = 0.16$, the (3+1)D CLVisc hydrodynamics can roughly describe the Au+Au data, while it underestimates the LHC measurements. Figure 3 (bottom panel) shows the similar results, but for r_3 . Unlike r_2 , the difference between higher energy and lower energy shows a weak centrality dependence. The (3+1)D CLVisc ideal hydrodynamic calculations still slightly overestimate the decorrelation effect at RHIC energy. With a viscous correction, the hydrodynamic calculations suggest an even stronger decorrelation for r_3 [8]. The results indicate the decorrelation is not only an initial-state effect, but also sensitive to the dynamical evolution of the collision system.

4. Conclusion

Measurements of longitudinal flow correlations for charged particles are presented in the pseudorapidity range $|\eta| < 1$ using a reference detector at $2.5 < \eta_{\text{ref}} < 4$ in Au+Au collisions at $\sqrt{s_{NN}} = 200 \text{ GeV}$ with the STAR detector at RHIC. The factorization of two-particle azimuthal correlations into single-particle flow harmonics, V_n , is found to be broken, and the amount of factorization breakdown increases approximately linearly as a function of the η separation between the two particles. The strength of the decorrelation is nearly independent of centrality for r_3 . However, for r_2 , the effect has a strong centrality dependence and is weakest in midcentral collisions. The results are compared with those from LHC and calculations from hydrodynamic models. The effect shows clear energy dependence and it is stronger for lower energies. The (3+1)D ideal hydrodynamics overestimates the decorrelation effect at RHIC energies. With a viscous

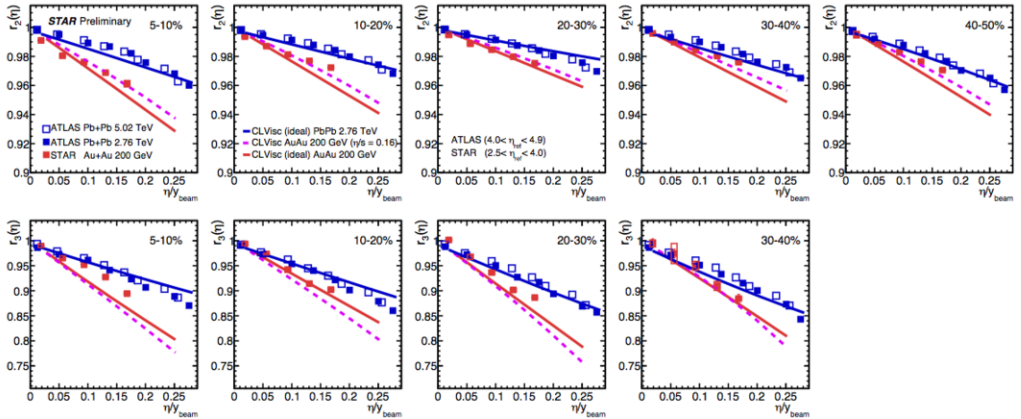


Fig. 3. $r_n(\eta)$ as a function of the normalized rapidity, and compared with three collision energies. Each panel shows results from one centrality interval. The error bars and hollowed boxes are statistical and systematic uncertainties, respectively. The top row shows the results for $r_2(\eta)$, and the bottom row shows those for $r_3(\eta)$.

correction, it can better describe r_2 , while it suggests an even larger r_3 . The results provide new constraints on both the initial-state geometry fluctuations and final-state dynamics of heavy-ion collisions.

5. Acknowledgements

This work is supported by the Major State Basic Research Development Program in China under Grant No. 2014CB845404, the National Natural Science Foundation of China under Grants No. 11522547, 11375251, and 11421505, NSF under grant numbers PHY-1305037 and PHY-1613294.

References

- [1] P. Bozek, W. Broniowski, J. Moreira, Phys. Rev. C 83 (2011) 034911.
- [2] K. Xiao, F. Liu, F. Wang, Phys. Rev. C 87 (2013) 011901.
- [3] J. Jia, P. Huo, Phys. Rev. C 90 (2014) 034915.
- [4] V. Khachatryan, et al., Phys. Rev. C 92 (2015) 034911.
- [5] M. Aaboud, et al., Eur. Phys. J. C 78 (2018) 142.
- [6] L.-G. Pang, H. Petersen, G.-Y. Qin, V. Roy, X.-N. Wang, Eur. Phys. J. A 52 (2016) 97.
- [7] L.-G. Pang, Y. Hatta, X.-N. Wang, B.-W. Xiao, Phys. Rev. D 91 (2015) 074027.
- [8] L.-G. Pang, H. Petersen, X.-N. Wang, Phys. Rev. C 97 (2018) 064918.